

Comparison of mechanical and microstructural behaviors of tungsten inert gas welded and friction stir welded dissimilar aluminum alloys AA 2014 and AA 5083

S. Sayer^{1*}, Ç. Yeni², O. Ertuğrul³

¹*Ege University, Ege Vocational School, 350 40 Bornova-Izmir, Izmir, Turkey*

²*Dokuz Eylül University, Faculty of Engineering, Department of Mechanical Engineering, Izmir, Turkey*

³*Dokuz Eylül University, Faculty of Engineering, Department of Materials and Metallurgical Engineering, Izmir, Turkey*

Received 13 January 2010, received in revised form 19 May 2010, accepted 25 August 2010

Abstract

In this study, dissimilar aluminum alloys 2014 and 5083 have been welded using two different welding methods, namely the solid state joining method friction stir welding (FSW), and the fusion welding method tungsten inert gas welding (TIG). The joint has been investigated in terms of its microstructure, hardness and mechanical properties. Optical microscopy was used to characterize the microstructure of the weld area. Microstructural examination reveals that a fine grain structure is formed in the nugget zone of FSW as a result of recrystallization and that they are smaller in size compared to the grains in the weld center of TIG, where grain growth has been observed due to heat input. The tensile testing results show that among the two welding methods employed, FSW has yielded better mechanical properties. The mechanical strength of the dissimilar joint, both in terms of yield and ultimate tensile strengths using FSW was found to be varying for aluminum alloys 2014 and 5083 between 60 % to values matching those of the base metal values, respectively. The results show that FSW can better suit to the joining of dissimilar aluminum alloys compared to TIG welding.

Key words: friction stir welding (FSW), tungsten inert gas (TIG), dissimilar joint, aluminum alloys 2014-5083, microstructure, mechanical properties

1. Introduction

Friction stir welding (FSW) is an innovative joining process, patented at The Welding Institute (TWI) in 1991 by Thomas et al. [1]. FSW uses a rotating (non-consumable) cylindrical tool that consists of a shoulder and a pin. The shoulder is pressed against the surface of the materials being welded, while the pin is forced between the two components by a downward force. The rotation of the tool under this force generates a frictional heat that decreases the resistance to plastic solid-state joining process; therefore, welding takes place below the melting point of the material. The softened material then easily moves behind the tool and forms a solid state weld as the stirred material is consolidated [2]. The FSW joint is created by friction heating with simultaneous severe plastic deformation of the weld zone material. Since the amount

of heat supplied is smaller than during fusion welding, heat distortions are reduced, thereby reducing the amount of residual stresses [3]. Moreover, consumable filler material, shielding gas or edge preparation are normally not necessary with FSW [4, 5].

Crucial aspects met in the welding of Al alloys are the presence of the brittle solidification phases and possible porosity formation subsequent to fusion welding; these problems are generally overcome by the FSW technique [6–9]. With no melting, the cast microstructure formed during conventional fusion welding, as well as the weld zone shrink from solidification are avoided.

Currently, FSW is mainly used to join similar materials; but so far, few systematic studies have been carried out to observe the effect due to dissimilarity [10, 11]. Welding of dissimilar materials is critical for several industrial sectors since many applications re-

*Corresponding author: tel.: +90(232) 343 66 00/7026; e-mail address: sami.sayer@ege.edu.tr

Table 1. Chemical compositions of AA 2014, AA 5083 (wt.%) and filler rod 4043 for TIG welding

Materials	Mg	Cu	Si	Mn	Cr	Fe	Others	Al
AA 2014	0.4	4.0	0.8	0.7	0.1	0.6	0.3	balance
AA 5083	4.2	0.1	0.4	0.6	0.2	0.3	0.4	balance
Filler rod 4043	0.05	0.04	4.9	–	–	0.2	0.25	balance

quire the use of more than one material. The absence of melting phase in FSW allows joining of dissimilar materials with the achievement of sound welds. Recent literature reports FS welding of several dissimilar aluminum alloys [12, 13], as well as between materials with extremely different mechanical and physical properties such as aluminum-steel, aluminum-magnesium and aluminum-silver [14–16]. Literature review also reveals that there is still lack of material property data regarding the comparison of FSW with TIG. Although it is observed that FSW, in general, yields stronger welds than fusion welds, more data is needed in order to support this fact. For the time being, few comparisons have been made of dissimilar materials welded by different methods [11–14].

The aim of the present study is to investigate the mechanical and microstructural properties achieved with FS butt welding and tungsten inert gas welding of dissimilar sheets, namely AA 2014 and AA 5083, which find use simultaneously in several industrial sectors owing to their distinct properties. AA 2014 is a heat treatable alloy with poor weldability properties, whereas AA 5083 is a non heat treatable but a weldable alloy.

2. Experimental procedure

2.1. Material

AA 2014 is a heat treatable alloy with high mechanical and fatigue strength; it is mostly used in aircraft components, automotive and heavy machinery industries. AA 5083 is a high strength alloy with very good weldability and corrosion resistance, it finds usage in industries such as shipbuilding, automotive and pressure vessels. AA 2014 and AA 5083 base metal sheets used in this study are in T4 and T0 conditions, respectively. Both plates have been manufactured by extrusion with the same dimensions of $275 \times 150 \times 5 \text{ mm}^3$ (length, width, thickness). The chemical compositions of both Al alloys and filler rod 4043 used in TIG welding are given in Table 1.

2.2. Friction stir welding (FSW)

The longitudinal direction of the FSW line was parallel to the extrusion direction of the 2014 and 5083 alloys. The tool used in this study consisted of a

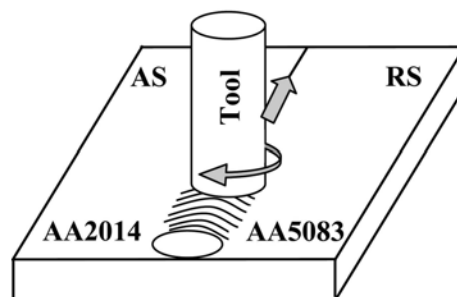


Fig. 1. Layout of the plates for FSW.

shoulder with a diameter of 20 mm and a pin with a diameter of 5 mm and a length of 4.7 mm. The FSW tool was fixed to the rotating axis of a milling machine; the tool was 3° tilted from the normal direction of the plate and rotated clockwise. Welding and rotation speeds were selected as 106 mm min^{-1} and 1600 rpm, respectively. The simultaneous rotational and translational motion of the welding tool during the welding process created a characteristic asymmetry between the adjoining sides. The side where the tool rotation coincides with the direction of the translation of the welding tool is called the advancing side (AS), while the other side, where the two motions, rotation and translation counteract is called the retreating side (RS) [17–20]. During friction stir welding, AA 2014 plate was fixed so as to be in the AS and AA 5083 to be in the RS, Fig. 1.

2.3. Tungsten inert gas welding (TIG)

The longitudinal direction of the TIG weld was taken parallel to the extrusion direction of dissimilar aluminum alloys AA 2014 and AA 5083. The abutting surfaces were cleaned before welding with a steel brush followed by light sanding with 400 grit SiC paper and degreasing with acetone. The cleaning media contained no carbon. A gap of 2 mm was left between the two plates being welded; a V joint configuration has been prepared. A ceramic base has been placed under the plates during welding in order to reduce heat loss, obtain a more homogeneous heat distribution and avoid warpage of the plates. One sided TIG welding has been carried out in two passes, owing to the thickness of the plates. Layout of the plates during TIG welding is shown in Fig. 2 and the welding parameters are presented in Table 2.

Table 2. Process parameters for TIG welded dissimilar Al alloys AA 2014 and AA 5083

Process parameters for TIG welding	
Welding machine	Oerlikon Prestotig 300
Filler rod type	Magmaweld TAL 4043
Filler rod diameter (mm)	2.4
Current (A)	140 (root) – 150 (top)
Voltage (V)	14
Preheating (°C)	200
Shield gas	argon
Gas pressure (bar)	10
Gas flow rate (l min ⁻¹)	10

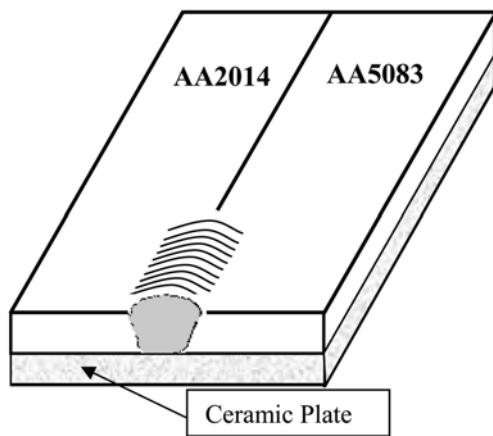


Fig. 2. Layout of the plates for TIG.

After welding with both methods, the joints were cross-sectioned perpendicular to the welding direction for metallographic analysis. The cut surfaces of the metallographic specimens were polished with alumina suspension; two different etching solutions were used in order to clearly establish the grain structure differences in dissimilar joints. In the first stage, the polished specimen has been etched for 20 s at 50°C in 100 ml water, 2 g sodium hydroxide acid solution and AA 2014 side has been examined for microstructural variations. In the second stage, the repolished specimen has been etched for 120 s at 25°C in 50 ml methyl alcohol, 30 ml hydrochloric acid, 25 ml nitric acid and one drop hydrofluoric acid solution to reveal the microstructural variations at the AA 5083 side. The microstructural features of the welds were investigated using an optical microscope. SEM images were used for the investigation of fracture surfaces.

The Vickers hardness profiles of the welded zones have been obtained at the weld cross-section using a Vickers indenter with 100 gf load applied for 10 s. Hardness measurements have been carried out transverse to the welding direction and along the middle section of the joints.

Tensile tests have been performed in order to evaluate the mechanical properties of the welded joints. Tensile tests were carried out at room temperature at a crosshead speed of 1 mm min⁻¹ using a computer-controlled testing machine. The tensile specimens were cut out perpendicular to the weld axis. Tensile tests are carried out according to ASTM E8-95a standard code.

3. Results and discussion

3.1. Microstructure

In the present study, dissimilar AA 2014 and 5083 have been successfully joined using the FSW and TIG processes and no visible porosity or macroscopic defects have been observed on the weld cross-section. The FSW process applied on dissimilar 2014 and 5083 aluminum alloys revealed the classical formation of the elliptical “onion ring” structure in the weld region. Four distinct zones are observed in FSW, namely the Nugget Zone (NZ), Thermomechanically Affected Zone (TMAZ), Heat Affected Zone (HAZ) and the Base Metal (BM). TIG welding, on the other hand, reveals three zones, namely the Weld Center, HAZ and the BM, which are typical in fusion welding.

Microstructural examinations are conducted at the middle sections of the specimens. In FSW welds, the NZ is the region that experiences the highest strain and undergoes recrystallization. The formation of such microstructure is due to the mechanical action of the tool probe that generates a continuous dynamic recrystallization process. The higher temperature and the severe plastic deformation during welding in the NZ result in a renewed fine grain structure [21]. Figure 3 shows the macrosection and the microstructures of several zones obtained by FS welding. Figure 3c shows the NZ, by moving towards the base metals, adjacent to the Nugget Zone, there lies the TMAZ and HAZ (Fig. 3b for AA 2014 and Fig. 3d for AA 5083). The TMAZ is the region surrounding the nugget on either side where there is less heat generation compared to the weld center and, therefore, may exhibit partial recrystallization [22]. In the HAZ the material progressively tends to remain unaffected [23]. Adjacent to the HAZ, there lies the BM (Fig. 3a for AA 2014 and Fig. 3e for AA 5083). From the different etching response of each material AA 2014 appears in darker color than AA 5083. The BM has long-equiaxed grains oriented along the rolling direction, whereas the weld nugget is composed of fine-equiaxed grains, approximately 5–8 μm in diameter, due to recrystallization, which are formed under high temperature and plastic deformation in the weld center due to the stirring process, which is in agreement with literature, Fig. 3c [24–26].

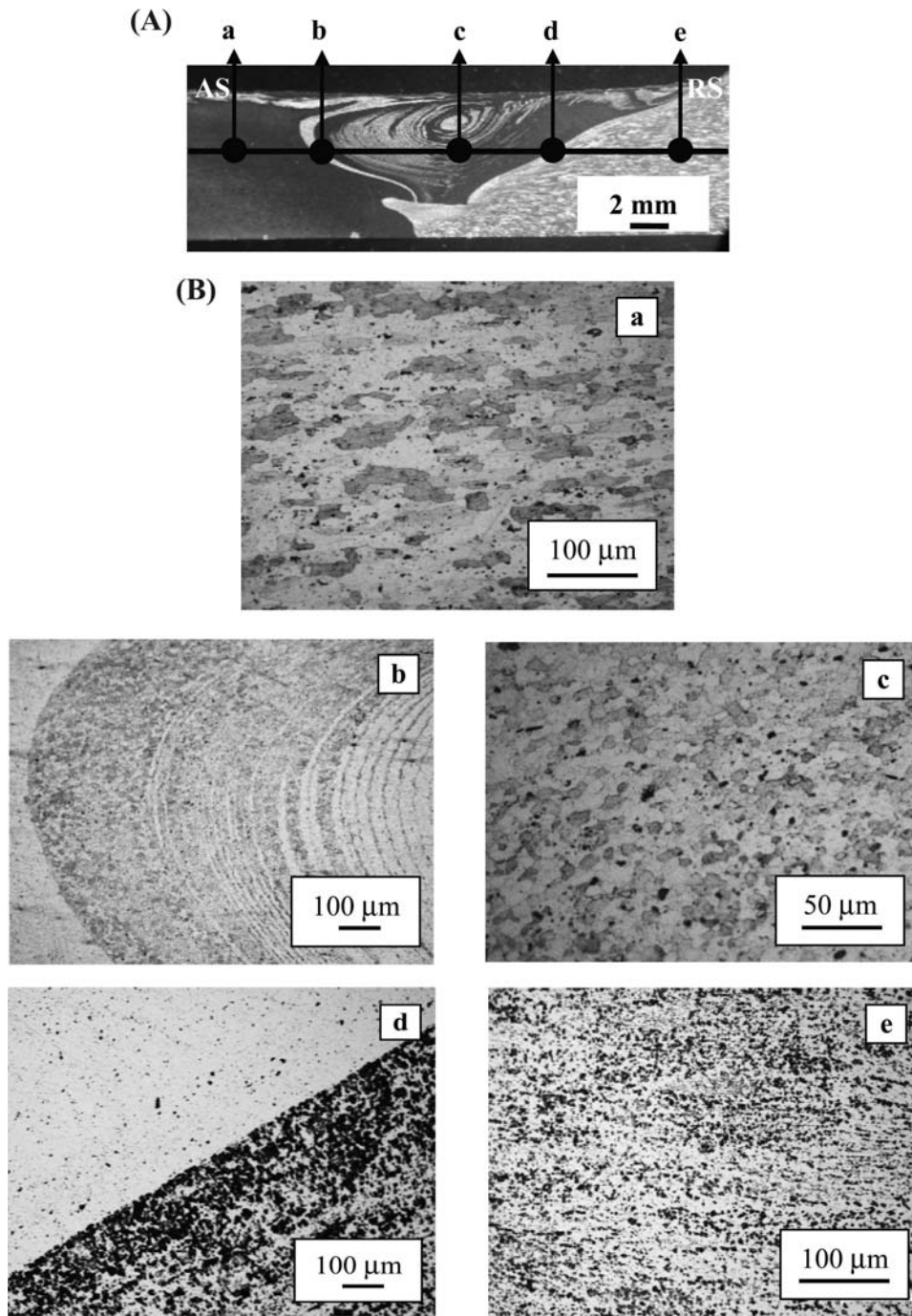


Fig. 3. FS weld region macrostructure and microstructures of (a) BM AA 2014, (b) TMAZ & HAZ AA 2014, (c) NZ AA 2014 & AA 5083, (d) TMAZ & HAZ AA 5083, (e) BM AA 5083.

Figure 4 shows the macrosection and the microstructures of several zones obtained by TIG welding. For TIG welds, the micrographs are taken from the second weld pass. In TIG welds, grains show a tendency of having greater diameters in the HAZ and weld region compared to the base metal due to high heat input to the material. In the HAZs, Figs. 4b and 4d, the grains become less equiaxed and in the weld region there is a nonhomogeneous and unequiaxed grain dis-

tribution. Grain sizes are measured about $25\ \mu\text{m}$ in diameter in the weld center, Fig. 4c.

Comparison of grain structures at the weld centers of FSW and TIG reveals that grain sizes have reduced in FSW due to recrystallization, whereas there is grain size increase in TIG due to severe heat input.

Investigation of fracture surfaces by SEM, Fig. 5, shows that in FS welds, the specimens are broken in a ductile manner at the interface of HAZ and the BM

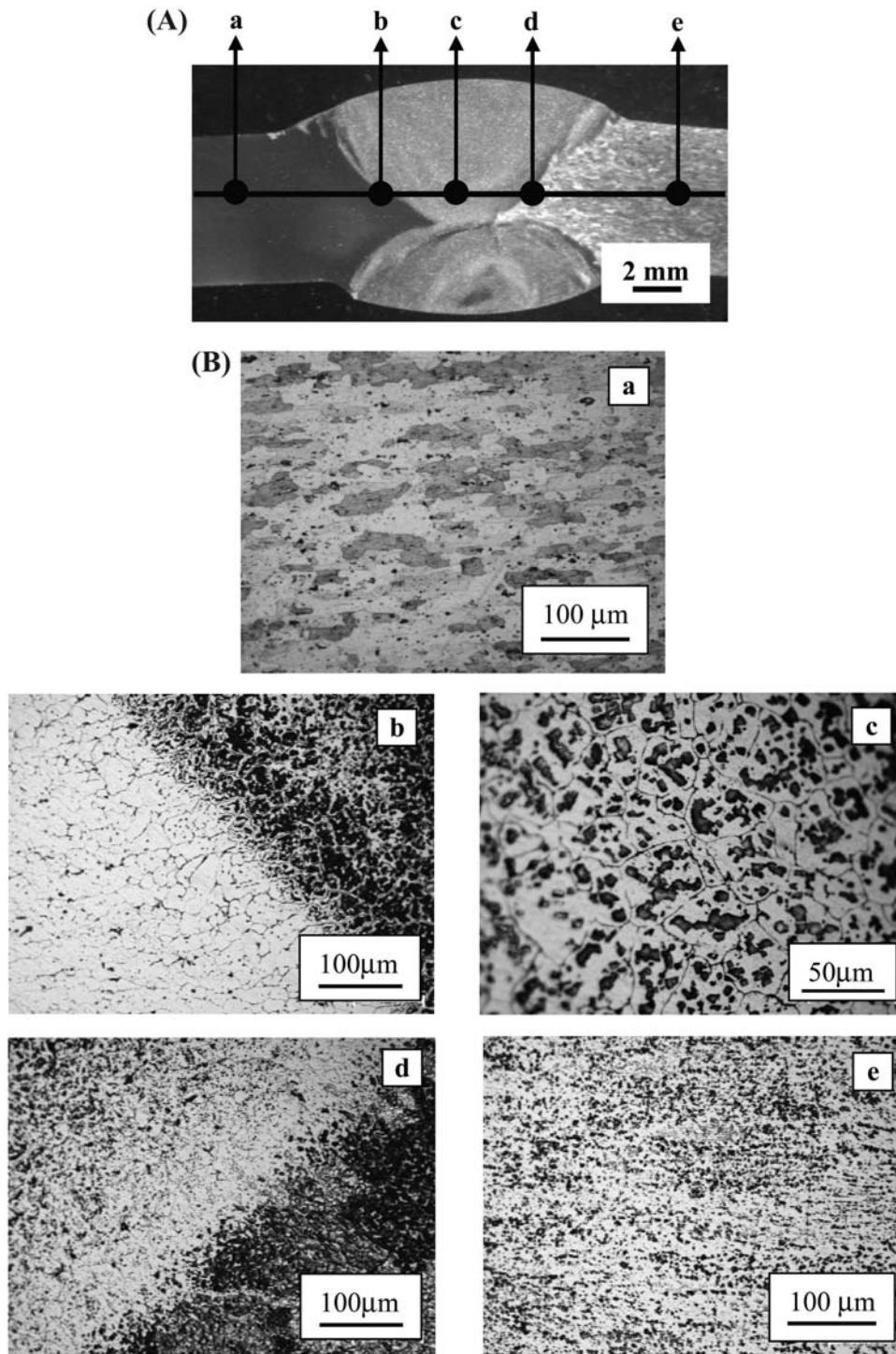


Fig. 4. TIG weld region macrostructure and microstructures of (a) BM AA 2014, (b) HAZ AA 2014, (c) Weld Center AA 2014 & AA 5083, (d) HAZ AA 5083, (e) BM AA 5083.

region. Fracture surfaces reveal microscopic voids of various sizes and shapes. As seen in Fig. 5a, a fairly homogeneous dimpled structure is observed. Dimples, likely to be associated with precipitates combined with ductile mechanisms, accelerate fracture. Brittle fracture dominates TIG welds with the fracture zone located in the weld center, Fig. 5b.

3.2. Hardness

Figure 6 shows the microhardness distribution over the weld cross section of welded dissimilar AA 2014 and AA 5083. BM hardness values of AA 2014 and AA 5083 are around 110 HV and 70 HV, respectively. In general, the FS welding process softens the

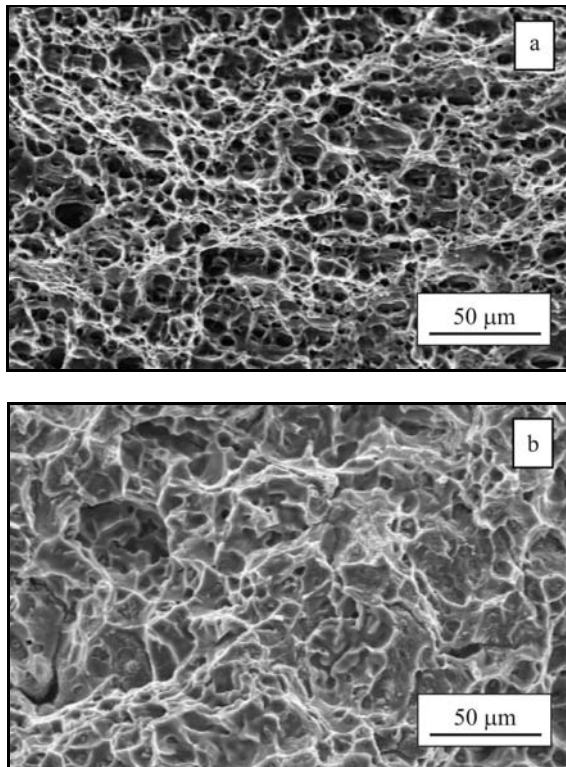


Fig. 5. Fracture surfaces (a) FSW, (b) TIG.

material within the weld region composed of HAZ and TMAZ, therefore reduces the hardness due to coarsening caused by thermomechanical conditions [14], whereas recrystallization due to extreme plastic deformation causes hardness increase in the NZ. On the other hand, the variation of the concentration of alloying elements in the nugget zone can be attributed to the variation of hardness values for dissimilar FSW, as in agreement with [15]. In the nugget zone, the region equal in width to the pin diameter, both hardness increase (on AA 2014 side) and decrease (on AA 5083 side) have been observed in this study. The nugget hardness recovery for AA 2014 is due to recrystallization of a very fine grain structure, this is in accordance with the classical behavior of aluminum alloys welded by FSW [13]. On the contrary, there is first hardness decrease at the AA 5083 side in the nugget zone followed by hardness increase going towards the TMAZ zone. Although there is recrystallization in this region, the hardness decrease can mostly be attributed to the mixing of the softer AA 5083 material into the complex structured nugget zone. The hardness increase followed by this decrease can be attributed to the stirring of harder AA 2014 to the softer AA 5083. The lowest hardness values are measured at the HAZ and TMAZ on AS side (AA 2014 side) as about 95 HV and for the RS side (AA 5083 side) as about 70 HV.

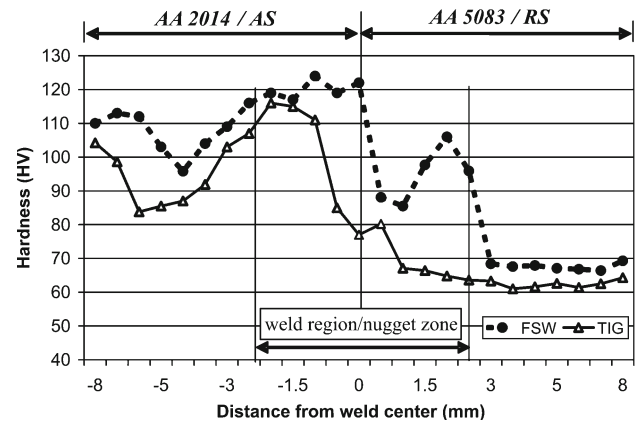


Fig. 6. Hardness profiles of dissimilar Al alloy AA 2014 and AA 5083 welded by TIG, and FSW.

Hardness measurements for TIG welding clearly indicate that TIG hardness values are less than those for FSW. On the HAZ region of AA 2014 side, a sharp hardness decrease to about 84 HV has been observed due to severe heat input. Hardness increases in the weld region on the AA 2014 side followed by a decrease at the weld center; this can be explained by the high Si content in the filler material. No significant hardness decrease, as seen in AA 2014, is observed in the HAZ region of AA 5083, which is a much softer material. For AA 5083 in T0 condition, there will normally be no effect of the thermal transient. The material is already as soft as it can be, and further heating does not lower its hardness. These findings are in agreement with existing literature [24].

3.3. Tensile properties

The tensile property values are obtained as the average of minimum three tests. FS welded specimens have been fractured on the AA 5083 HAZ base metal interface. BM and dissimilar FSW and TIG tensile properties are presented in Table 3. Table 3 reveals that tensile strength values of FS welds are lower than those for AA 2014 BM (60 %) and slightly overmatching with those of AA 5083 BM (104 %). Since AA 5083 is in T0 condition, the properties in the weld region are similar to those in the base metal. Literature review suggests that depending on the nugget grain size, there may be some strength increment due to microstructural refinement [24, 27, 28]. This fact is in agreement with our findings.

For TIG welding, the tensile strength value of the weld region is lower than both BM values (42 % and 74 % for AA 2014 and AA 5083, respectively). TIG welded specimens have fracture in the weld region. Since the FS welded dissimilar joint showed lower or even matching tensile properties compared to base metal values, the results can be considered quite sat-

Table 3. Tensile properties of the BM and dissimilar TIG and FSW welded AA 2014 & AA 5083 joints

Material/Process		Yield strength $R_{p0.2}$ (MPa)	Ultimate tensile strength R_m (MPa)	Total elongation (%)	Joint efficiency in terms of R_m (%)
BM	AA 2014	282	412	17.2	–
	AA 5083	130	237	16.4	–
TIG	AA 2014 – AA 5083	128	175	2.6	0.42–0.74
FSW	AA 2014 – AA 5083	139	247	7.1	0.6–1.04

isfactory taking into account the drastic conditions to which the materials undergo during the friction stir process, in agreement with [13]. Tensile results reveal that dissimilar Al alloys possess better mechanical properties when welded with FSW rather than TIG welding, as supported by the hardness distribution.

4. Conclusions

Two dissimilar aluminum alloys, namely, AA 5059 and AA 7075 were friction stir welded by using a welding speed of 100 mm min^{-1} and a rotation speed of 1600 rpm. The following conclusions can be derived from this study:

1. Both welding methods, FSW and TIG, were applied successfully to dissimilar AA 2014 and AA 5083 with no visible porosity or macroscopic defects across the weld cross-section.

2. In FS welding, the NZ possessed fine-equiaxed grains due to recrystallization, compared to increased grain size in TIG due to severe heat input.

3. Tensile strength values for both welds were lower compared to base metal values with the exception of AA 5083 BM, which is even matching in FSW.

4. Tensile results reveal that, dissimilar Al alloys are better suited to be welded with FS process compared to high heat input fusion welding processes, such as TIG.

Acknowledgements

The authors would like to thank Res. Asst. M. Kuşoğlu and the Materials & Testing Laboratory Staff of Department of Materials-Metallurgy Engineering, Dokuz Eylül University, for their generous help in carrying out the measurements and evaluations. The authors are also grateful to Oerlikon Company, Manisa for their contribution to TIG welding.

References

- [1] THOMAS, W. M.—NICHOLAS, E. D.—NEEDHAM, J. C.—MURCH, M. G.—TEMPLESMITH, P.—DAWES, C. J.: International Patent Application No. PCT/GB92/02203.
- [2] SCIALPI, A.—DE GIORGI, M.—DE FILIPPIS, L. A. C.—NOBILE, R.—PANELLA, F. W.: *Materials and Design*, 29, 2008, p. 928. doi:10.1016/j.matdes.2007.04.006
- [3] THOMAS, W. M.—NICHOLAS, E. D.: *Materials and Design*, 18, 1997, p. 269. doi:10.1016/S0261-3069(97)00062-9
- [4] SHIGEMATSU, I.—KWON, Y. J.—SUZUKI, K.—IMAI, T.—SAITO, N.: *Journal of Mat. Science Lett.*, 22, 2003, p. 353. doi:10.1023/A:1022688908885
- [5] LEE, W. B.—YEON, Y. M.—JUNG, S. B.: *Scripta Materialia*, 49, 2003, p. 423. doi:10.1016/S1359-6462(03)00301-4
- [6] SATO, Y. S.—URATA, M.—KOKAWA, H.—IKEDA, K.: *Mat. Science and Eng., A354*, 2003, p. 298. doi:10.1016/S0921-5093(03)00008-X
- [7] BERBON, P. B.—BINGEL, W. H.—MISHRA, R. S.—BAMPTON, C. C.—MAHONEY, M. W.: *Scripta Materialia*, 44, 2001, p. 61. doi:10.1016/S1359-6462(00)00578-9
- [8] LEE, W. B.—YEON, Y. M.—JUNG, S. B.: *Mat. Science and Eng., A355*, 2003, p. 154. doi:10.1016/S0921-5093(03)00053-4
- [9] KNIPTRÖM, K. E.: *New Welding Methods for Aluminium*, Svetsaren, 3, 1995, p. 5.
- [10] WERT, J. A.: *Scripta Materialia*, 49, 2003, p. 607. doi:10.1016/S1359-6462(03)00215-X
- [11] MORABITO, A. E.: *Thermomechanical Analysis of Thermoelastic and Dissipative Effect Associated with the Fatigue Behavior of Aluminum Alloy 2024 T3*. [Ph.D. Thesis]. Lecce, Università del Salento 2003.
- [12] SRINIVASAN, B. P.—DIETZEL, W.—ZETTLER, R.—DOS SANTOS, J. F.—SIVAN, V.: *Mater. Sci. Eng., A* 392, 2005, p. 292. doi:10.1016/j.msea.2004.09.065
- [13] CAVALIERE, P.—NOBILE, R.—PANELLA, F. W.—SQUILLACE, A.: *Inter. Journal of Machine Tools & Manufacture*, 46, 2006, p. 588.
- [14] UZUN, H.—DONE, C. D.—ARGAGNOTTO, A.—GHIDINI, T.—AMBARO, C.: *Materials and Design*, 26, 2005, p. 41.
- [15] CHEN, C. M.—KOVACEVIC, R.: *Inter. Journal of Machine Tools & Man.*, 44, 2004, p. 1205.
- [16] SOMASEKHARAN, A. C.—MURR, L. E.: *Mater. Charact.*, 52, 2004, p. 49. doi:10.1016/j.matchar.2004.03.005
- [17] ERICSSON, M.—SANDSTRÖM, R.: *International Journal of Fatigue*, 25, 2003, p. 1379.
- [18] HAAGENSEN, P. J.—MIDLING, O. T.—RANES, M.: *Fatigue performance of friction stir butt welds in*

- a 6000 series aluminum alloy. Boston, Computational Mechanics Publications, 1995, p. 225.
- [19] HAGSTRÖM, J.—SANDSTRÖM, R.: Materials Science Forum, 217–222, 1996, p. 1727.
- [20] ZHOU, C.—YANG, X.—LUEN, G.: Scripta Mater., 53, 2005, 1187.
- [21] HASSAN, K. A. A.—NORMAN, A. F.—PRICE, D. A.—PRANGNELL, P. B.: Acta Mater., 51, 2003, p. 1923. [doi:10.1016/S1359-6454\(02\)00598-0](https://doi.org/10.1016/S1359-6454(02)00598-0)
- [22] LIU, G.—MURR, L. E.—NIOU, C. S.—CLURE, J. C.—VEGA, F. R.: Scripta Materialia, 37, 1997, p. 355.
- [23] SU, J. Q.—NELSON, T. W.—STERLING, C.: Materials Science and Engineering A, 405, 2005, p. 277. [doi:10.1016/j.msea.2005.06.009](https://doi.org/10.1016/j.msea.2005.06.009)
- [24] MAHONEY, M. W.—MISHRA, R. S.—NELSON, T.: Friction Stir Welding and Processing. Warrendale, PA, USA, TMS 2001, p. 183.
- [25] SAYER, S.—CEYHUN, V.—TEZCAN, O.: Kovove Mater., 46, 2008, p. 157.
- [26] YENİ, Ç.: Practical Metallurgy, 45, 2008, p. 8.
- [27] KARLSSON, L.—SVENSSON, L.—LARSSON, H.: In: Proc. of the 5th Int. Conf. Eds.: Vitek, J. et al. Materials Park, OH, ASM International 1999, p. 574.
- [28] SATO, Y. S.—HWAN, S.—PARK, C.—KOKAWA, H.: Metall. Mater. Trans. A, 32, 2003, p. 3033. [doi:10.1007/s11661-001-0178-7](https://doi.org/10.1007/s11661-001-0178-7)